

Scaling Exponents in Anisotropic Hydrodynamic Turbulence

Victor S. L'vov, Itamar Procaccia and Vasil Tiberkevich

Department of Chemical Physics, The Weizmann Institute of Science, Rehovot 76100, Israel

^yRadiophysical Faculty, National Taras Shevchenko University of Kiev, Kiev, Ukraine

In anisotropic turbulence the correlation functions are decomposed in the irreducible representations of the $SO(3)$ symmetry group (with different "angular momenta"). For different values of ℓ the second order correlation function is characterized by different scaling exponents $\zeta_\ell(\ell)$. In this paper we compute these scaling exponents in a Direct Interaction Approximation (DIA). By linearizing the DIA equations in small anisotropy we set up a linear operator and find its zero-modes in the inertial interval of scales. Thus the scaling exponents in each ℓ -sector follow from solvability condition, and are not determined by dimensional analysis. The main result of our calculation is that the scaling exponents $\zeta_\ell(\ell)$ form a strictly increasing spectrum at least until $\ell = 6$, guaranteeing that the effects of anisotropy decay as power laws when the scale of observation diminishes. The results of our calculations are compared to available experiments and simulations.

I. INTRODUCTION

All realistic turbulent flows are maintained by anisotropic (and inhomogeneous) forcing. Thus the principal conceptual model of turbulence, i.e. "homogeneous isotropic turbulence", exists only in theory. Testing theoretical predictions that are derived on the basis of such a model in experimental flows (or in simulations) that are patently anisotropic can sometimes lead to premature or erroneous conclusions about important issues like the universality of scaling exponents and other fundamental issues in the theory of turbulence. The justification for disregarding the effects of anisotropy was the old conjecture that in the limit of very high Reynolds numbers and very small scales, local isotropy may be restored by the non-linear transfer mechanism that cascades energy from large to small scales. In the last decade there had been a number of observations that claimed the opposite [1, 2, 3]. On the whole, these observations were based on measuring objects that "should vanish" for isotropic flows, and observing their behavior as a function of Reynolds number (Re) or scale. Thus for example objects made of the normal derivative of the downstream velocity components were examined:

$$S_{2k+1} = \frac{\overline{h(\partial u_x = \partial y)^{2k+1} i}}{\overline{h(\partial u_x = \partial y)^2 i^{k+1=2}}} ; \quad (1)$$

The pointed brackets denote ensemble average, u_x is the streamwise component of the Eulerian velocity field $u(r)$, and y is in the spanwise direction. Since such objects vanish in isotropic systems, their increase as a function of Re were interpreted as a lack of restoration of local isotropy. The problem with such measures is that objects of this type are also sensitive to the phenomenon of intermittency, and also perfectly isotropic objects like

$$K_{2k+1} = \frac{\overline{h(\partial u_x = \partial x)^{2k+1} i}}{\overline{h(\partial u_x = \partial x)^2 i^{k+1=2}}} ; \quad (2)$$

increase with Reynolds number. It is thus unclear what is the more important source of the observation that the

objects (1) do not vanish even when the Reynolds number is increased.

Until rather recently it was not obvious how to assess the anisotropic effects in a clear fashion, separating the contributions of the isotropic sector from the rest. Starting with [4], it was proposed that one can do so usefully by finding systematically the projections of the measured correlation or structure functions on the irreducible representations of the $SO(3)$ group of all rotations. This approach was found useful in analyzing experimental results [5, 6, 7] and numerical simulations [8, 9]. In the context of passive scalar and passive scalar advection it gave rise to a number of exact results [10, 11, 12]. In its simplest form the projection is applied to the p th order structure functions (with $\hat{R} = R = R \hat{R}^j$):

$$S_p(R) = \overline{h u(x+R) u(x) \hat{R}^{i_p} i} ; \quad (3)$$

Such objects admit a relatively simple $SO(3)$ decomposition since they are scalar objects. We can thus span them by the usual spherical harmonics:

$$S_p(R) = \sum_{\ell=0}^{\infty} \sum_{m=-\ell}^{\ell} S_p^m(R) Y_m(\hat{R}) ; \quad (4)$$

In this equation we have used the indices m to label, respectively, the total angular momentum and its projection along a reference axis, say \hat{z} . We are interested in particular in the scaling properties of the amplitudes $S_p^m(R)$,

$$S_p^m(R) \sim A_m R^{-\zeta_p(\ell)} ; \quad (5)$$

In the case of exactly soluble models [10, 11, 12] it was found that the scaling exponents $\zeta_p(\ell)$ form a strictly increasing spectrum as a function of ℓ . In such cases it becomes completely clear that for $R \neq 0$, which in the limit $Re \rightarrow \infty$ can still be in the inertial range, the higher order ℓ contributions disappear in favor of the isotropic contribution alone. Thus if one can demonstrate the existence of a strictly increasing spectrum of exponents also

in the context of the Navier-Stokes dynamics, one would establish that local isotropy is restored at the smallest scales when $Re \gg 1$ (i.e. when the viscous cut-off goes to zero). The numerical values of the scaling exponents will determine the rate (in scales) at which isotropy is restored. The aim of this paper is to present such a calculation.

A calculation of the second order anisotropic exponents $\zeta_2(\nu)$, based on the Navier-Stokes equations, was attempted before in [13]. The analysis there concentrated on the forced solutions for the second order structure function $S_2(R)$, and concluded with two sets of dimensional predictions. The first, assuming that the anisotropic forcing is analytic, reads

$$\zeta_2(\nu) = \nu + 2 = 3; \quad \text{forced solution, analytic:} \quad (6)$$

The second forced solution was computed for non-analytic forcing, resulting with

$$\zeta_2(\nu) = 4 = 3; \quad \text{forced solution, nonanalytic:} \quad (7)$$

Another, more phenomenological approach, was presented in [9], generalizing an earlier argument by Lumley [14]. In this approach one does not balance the energy transfer against the forcing, but rather invokes the existence of a shear $s_{ik} = \partial u_i / \partial x_k$ as the main reason for the anisotropy. Performing dimensional analysis in which the shear is added to ν , the mean energy flux per unit time and mass, one ends up with the prediction

$$\zeta_2(\nu) = \frac{2 + \nu}{3}; \quad \text{dimensional, shear dominated.} \quad (8)$$

We note that for $\nu = 2$ the predictions (7) and (8) coincide; all three predictions disagree for $\nu > 2$.

These predictions do not agree with the result of the only vector model with pressure that had been solved exactly, i.e. the "linear pressure model" [12]. This model captures some of the aspects of the pressure term in Navier-Stokes turbulence, while being linear and therefore much simpler problem. The non-linearity of the Navier-Stokes equation is replaced by an advecting field $w(x;t)$ and an advected field $v(x;t)$. The advecting field $w(x;t)$ is taken with known dynamics and statistics. Both fields are assumed incompressible. The equation of motion for the vector field $v(x;t)$ is:

$$\begin{aligned} \partial_t v + w \cdot \nabla v + \nabla p - \nabla^2 v &= f; \\ \nabla \cdot v &= 0; \quad \nabla \cdot w = 0; \end{aligned} \quad (9)$$

In this equation, $f(x;t)$ is a divergence free forcing term and ν the viscosity. The domain of the system is taken to be infinite. Following Kraichnan's model for passive scalar [15], the advecting field $w(x;t)$ is chosen to be a white-noise Gaussian process with a correlation function which is given by:

$$\begin{aligned} \langle w_i(x;t) w_j(x';t') \rangle &= D \delta_{ij} \delta(x-x') \delta(t-t'); \\ \langle w_i(x;t) \partial_{x_j} w_k(x';t') \rangle &= D \delta_{ik} \delta_{ij} \delta(x-x') \delta(t-t'); \\ \langle \partial_{x_j} w_i(x;t) \partial_{x_k} w_l(x';t') \rangle &= D \delta_{il} \delta_{jk} \delta(x-x') \delta(t-t'); \end{aligned} \quad (10)$$

$$= D R^{-\zeta_2} \left(\delta_{ij} + 2 \frac{R_i R_j}{R^2} \right); \quad (11)$$

The forcing $f(x;t)$ is also taken to be a Gaussian white noise process. Its correlation function is

$$\langle f_i(x;t) f_j(x';t') \rangle = \delta_{ij} \delta(x-x') \delta(t-t'); \quad (12)$$

The forcing is responsible for injecting energy and anisotropy to the system at an outer scale L . We choose the tensor function $F(x)$ to be analytic in x , anisotropic, and vanishing rapidly for $|x| \gg 1$.

To compare with the predictions (6) and (8) we should take $\nu = 4 = 3$ in Eq. (11). For this value of ν the result of [12] are the exponents $\zeta_2(0) = 2 = 3$, $\zeta_2(2) = 1.25226$, $\zeta_2(4) = 2.01922$, $\zeta_2(6) = 4.04843$, $\zeta_2(8) = 6.06860$ and $\zeta_2(10) = 8.08337$, in rather sharp disagreement with the predictions (6)–(8). We will see that the calculation presented below for the Navier-Stokes case comes up with results in close agreement with those of the linear pressure model. We thus will present a strong belief that the dimensional predictions (6)–(8) fail to capture the correct results for the Navier-Stokes case.

In our approach we start from the Navier-Stokes equations, and write down an approximate equation satisfied by the second order correlation function, in the Direct Interaction Approximation (DIA). This equation is non-linear. For a weakly anisotropic system we can linearize the equation, to define a linear operator over the space of the anisotropic components of the second order correlation function. The solution is then a combination of forced solutions and "zero modes" which are eigenfunctions of eigenvalue zero of the linear operator. The exponents of the forced solutions are identical to (6), but the exponents of the zero modes are smaller, and therefore leading with respect to form. The exponents (7) are not physical, and are not observed in experiments or simulations. The exponents of the zero modes are close to (8) for $\nu = 2$ and 4, but begin to deviate strongly for $\nu = 6$, falling very close to the predictions of the linear pressure model. We will argue that again the exponents of the zero modes are those that are observed in simulations.

The structure of the paper is as follows: in Sect. II we set up the DIA equations for the second order structure function, and linearize them in weak anisotropy. We present the symmetry properties of the resulting operator, to simplify as much as possible the SO(3) decomposition which is presented in Sect. III. The actual calculation of the scaling exponents is detailed in Sect. IV. Finally in Sect. V we present concluding remarks.

II. MODEL EQUATIONS FOR WEAK ANISOTROPY IN THE DIA APPROXIMATION

A. DIA equations

It is customary to discuss the DIA equations in $k;t$ representation. The Fourier transform of the velocity

field $u(r;t)$ is defined by

$$u(k;t) = \int dr \exp[i(r-k)]u(r;t) : \quad (13)$$

The Navier-Stokes equations for an incompressible fluid then read

$$\frac{\partial}{\partial t} + k^2 u(k;t) = \frac{i}{2} \int \frac{d^3 q d^3 p}{(2\pi)^3} (k+q+p)u(q;t)u(p;t) : \quad (14)$$

The interaction amplitude $\Phi(k)$ is defined by

$$\Phi(k) = P(k)k + P(k)k ; \quad (15)$$

with the transverse projection operator P defined as

$$P = \frac{k \cdot k}{k^2} : \quad (16)$$

The statistical object that is the concern of this paper is the second order (tensor) correlation function $F(k;t)$,

$$(2\pi)^3 F(k;t) = \langle u(k;t)u(q;t) \rangle : \quad (17)$$

In stationary conditions this object is time independent. Our aim is to find its k -dependence, especially in the anisotropic sectors.

It is well known that there is no close-form theory for the second order simultaneous correlation function. We therefore need to resort to standard approximations that lead to model equations. An approach that is by now time-honored is Kraichnan's DIA, which leads to the approximate equation of motion

$$\frac{\partial F}{\partial t}(k;t) = I(k;t) - k^2 F(k;t) ; \quad (18)$$

where

$$I(k) = \int \frac{d^3 q d^3 p}{(2\pi)^3} (k+p+q) \Phi(k;q;p) : \quad (19)$$

In this equation

$$\Phi(k;q;p) = \frac{1}{2} [\Phi(k;q;p) + \Phi(k;q;p)] ; \quad (20)$$

and

$$\begin{aligned} \Phi(k;q;p) &= \Phi(k;q;p) \Phi(k) \\ &+ \begin{bmatrix} \Phi(q)F(p)F(k) \\ \Phi(p)F(q)F(k) \\ \Phi(k)F(q)F(p) \end{bmatrix} : \quad (21) \end{aligned}$$

In stationary conditions and for k in the inertial range we need to solve the integralequation $I(k) = 0$.

The process leading to these equations is long; one starts with the Dyson-Wild perturbation theory, and truncates (without justification) at the first loop order.

In addition one asserts that the time dependence of the response function and the correlation functions are the same. Finally one assumes that the time correlation functions decay in time in a prescribed manner. This is the origin of the "triad interaction time" $\tau(k;q;p)$. If one assumes that all the correlation functions involved decay exponentially (i.e. like $\exp(-k\tau)$), then

$$\tau(k;q;p) = \frac{1}{k+q+p} : \quad (22)$$

For Gaussian decay, i.e. like $\exp[-(k\tau)^2]$,

$$\tau(k;q;p) = \frac{1}{k^2 + q^2 + p^2} : \quad (23)$$

All these approximations are uncontrolled. Nevertheless DIA is known to give roughly correct estimates of scaling exponents and even of coefficients. For the case at hand, where we are interested in scaling exponents that were never computed from first principle, it certainly pays to examine what this approach has to predict.

Eq. (19) poses a nonlinear integral equation which is closed once we model Φ . One may use the estimate $\Phi(k) = U_k$ where U_k is the typical velocity amplitude on the inverse scale of k , which is evaluated as $U_k^2 = k^3 F(k)$.

$$U_k = C k^{5/2} \frac{P}{F(k)} : \quad (24)$$

In isotropic turbulence Eqs. (19) and (24) have an exact solution with Kraichnan scaling exponents,

$$\begin{aligned} F_0(k) &= P(k)F(k) ; \\ F(k) &= C^{-2/3} k^{11/3} ; \quad U_k = C^{-1/3} k^{2/3} : \quad (25) \end{aligned}$$

Note that the scaling exponents in k -representation have a d -dependent difference from their numerical value in r -representation. In 3-dimensions $\nu = \nu + 3$, and the exponent $2/3$ turns to $11/3$ in Eq.(25).

For weak anisotropic turbulence Eq.(19) will pose a linear problem for the anisotropic components which depends on this isotropic solution.

B. DIA with Weak Anisotropy

In weakly anisotropic turbulence we consider a small anisotropic correction $f(k)$ to the fundamental isotropic background

$$F(k) = F_0(k) + f(k) : \quad (26)$$

The first term vanishes with the solution (25). Linearizing our integral equation with respect to the anisotropic correction we read

$$\begin{aligned} I(k) &= \int \frac{d^3 q d^3 p}{(2\pi)^3} (k+p+q) [\Phi(k;q;p)f(k) \\ &+ 2T(k;q;p)f(q)] = 0 ; \end{aligned}$$

$$\begin{aligned} S & \quad (k; q; p) = \frac{f(k; q; p)}{F(k)}; \\ T & \quad (k; q; p) = \frac{f(k; q; p)}{F(q)}; \end{aligned} \quad (27)$$

We reiterate that the functional derivatives in Eq.(27) are calculated in the isotropic ensemble. In computing these derivatives we should account also for the implicit dependence of $(k; q; p)$ on the correlation function through Eq. (24). We can rewrite Eq. (27) in a way that brings out explicitly the linear integral operator \hat{L} ,

$$\hat{L} f_i = \int \frac{d^3 q}{(2\pi)^3} L(k; q) f(q) = 0; \quad (28)$$

where the kernel of the operator is

$$\begin{aligned} L(k; q) &= \int \frac{d^3 p}{(2\pi)^3} S(k; p; k-p) \\ &+ 2T(k; q; k-q); \end{aligned} \quad (29)$$

C. Symmetry properties of the linear operator

The first observation to make is that the linear operator is invariant under all rotations. Accordingly we can block diagonalize it by expanding the anisotropic perturbation in the irreducible representation of the $SO(3)$ symmetry group. These have principal indices ℓ with an integer ℓ going from 0 to ∞ . The zeroth component is the isotropic sector. Correspondingly our integral equation takes the form

$$L(k) = L_0(k) + \sum_{\ell=1}^{\infty} L_{\ell}(k) = 0; \quad (30)$$

The block diagonalization implies that each ℓ -block provides an independent set of equations (for every value of k):

$$L_{\ell}(k) = 0; \quad (31)$$

The first term of (30) vanishes with the solution (25). For all higher values of ℓ we need to solve the corresponding equation

$$\hat{L} f_{\ell} = 0; \quad (32)$$

We can block diagonalize further by exploiting additional symmetries of the linear operator. In all our discussion we assume that our turbulent flow has zero helicity. Correspondingly all the correlation functions are invariant under the inversion of k :

$$F_0(k) = F_0(-k); \quad f_{\ell}(k) = f_{\ell}(-k); \quad (33)$$

Consequently there are no odd ℓ components, and we can write

$$f_{\ell}(k) = \sum_{j=2,4,\dots}^{\ell} f_{\ell j}(k); \quad (34)$$

We also note that in general $u(k) = u(-k)$. Accordingly, the correlation functions are real. From this fact and the definition it follows that the correlation functions are symmetric to index permutation,

$$F_0(k) = F_0(-k); \quad f_{\ell}(k) = f_{\ell}(-k); \quad (35)$$

As a result our linear operator is invariant to permuting the first $(i; j)$ and separately the second $(k; l)$ pairs of indices. In addition, the operator is symmetric to $k \leftrightarrow -k$ together with $q \leftrightarrow -q$. This follows from the symmetry (33) and from the appearance of products of two interaction amplitudes (which are antisymmetric under the inversion of all wave-vectors by themselves).

Finally, our kernel is a homogeneous function of the wavevectors, meaning that in every block we can expand in terms of basis functions that have a definite scaling behavior, being proportional to k^{-2} .

III. $SO(3)$ DECOMPOSITION

As a result of the symmetry properties the operator \hat{L} is block diagonalized by tensors that have the following properties:

They belong to a definite sector $(\ell; m)$ of the $SO(3)$ group.

They have a definite scaling behavior, i.e., are proportional to k^{-2} with some scaling exponent α .

They are either symmetric or antisymmetric under permutations of indices.

They are either even or odd in k .

In [10] we discuss these types of tensors in detail. Here we only quote the final results. In every sector $(\ell; m)$ of the rotation group with $\ell > 1$, one can find 9 independent tensors $X_{\ell}(k)$ that scale like $k^{-2(\ell)}$. They are given by $k^{-2(\ell)} B_{j, \ell}^{(\ell)}(\hat{k})$, where the index j runs from 1 to 9, enumerating the different spherical tensors. The unit vector $\hat{k} = k/k$. These nine tensors can be further subdivided into four subsets:

Subset I of 4 symmetric tensors with $(-)^{\ell}$ parity.

Subset II of 2 symmetric tensors with $(-)^{\ell-1}$ parity.

Subset III of 2 antisymmetric tensors with $(-)^{\ell-1}$ parity.

Subset IV of 1 antisymmetric tensor with $(-)^{\ell}$ parity.

Due to the diagonalization of \hat{L} by these subsets, the equation for the zero modes foliates, and we can compute the zero modes in each subset separately. In this paper,

we choose to focus on subset I, which has the richest structure. The four tensors in this subset are given by

$$\begin{aligned} E_{1,m}(\hat{k}) &= k^{-2} k k_{} (k); \\ E_{2,m}(\hat{k}) &= k^{-1} [k_{\theta} + k_{\phi}] (k); \\ E_{3,m}(\hat{k}) &= k^{-1} (k); \\ E_{4,m}(\hat{k}) &= k^{-1/2} \theta \theta (k); \end{aligned} \quad (36)$$

where $ (k)$ are the standard spherical harmonics. We expect the calculation of the other subsets to be easier.

The last property to employ is the incompressibility of our target function $f(\hat{k})$. Examining the basis (37) we note that we can find two linear combinations that are transverse to k and two linear combinations that are longitudinal in k . We need only the former, which have the form

$$\begin{aligned} B_{1,m}(\hat{k}) &= k^{-1} P_{}(k) (k); \\ B_{2,m}(\hat{k}) &= k^{-1} [k^2 \theta \theta - (- 1)(k_{\theta} + k_{\phi}) \\ &\quad + (- 1)] (k); \end{aligned} \quad (37)$$

Using this basis we can now expand our target function as

$$f(\hat{k}) = k^{-2()} c_1 B_{1,m}(\hat{k}) + c_2 B_{2,m}(\hat{k}) \quad (38)$$

IV. CALCULATION OF THE SCALING EXPONENTS

Substituting Eq.(38) into Eq.(32) we find

$$\hat{L} q^{-2()} \mathfrak{B}_{1,m} i c_1 + \hat{L} q^{-2()} \mathfrak{B}_{2,m} i c_2 = 0 \quad (39)$$

Projecting this equation on the two functions of the basis (37) we obtain a matrix

$$\begin{aligned} L_{ij}(; 2()) &= \int d\hat{k} B_{i,m}(\hat{k}) \hat{L} q^{-2()} \mathfrak{B}_{j,m} i \\ &= \frac{d^3 q}{(2)^3} \int d\hat{k} B_{i,m}(\hat{k}) L(\hat{k}; q) q^{-2()} B_{j,m}(q); \end{aligned} \quad (40)$$

Here we have full integration with respect to q , but only angular integration with respect to k . Thus the matrix depends on k as a power, but we are not interested in this dependence since we demand the solvability condition

$$\det L_{ij}(; 2()) = 0 \quad (41)$$

It is important to stress that in spite of the explicit m dependence of the basis functions, the matrix obtained in this way has no m dependence. In the calculation below we can therefore put, without loss of generality, $m = 0$. This is like having cylindrical symmetry with a symmetry axis in the direction of the unit vector \hat{n} . In

this case we can write the matrix $B_{ij}(\hat{k})$ (in the vector space $ = x; y; z$) as

$$B_{ij}(\hat{k}) = k^{-1} \hat{B}_{ij,\hat{k}}(k^{-1} P_{}(\hat{k} \cdot \hat{n})); \quad (42)$$

where $\hat{B}_{ij,\hat{k}}$ are matrix operators, acting on wave vector k :

$$\begin{aligned} \hat{B}_{1,\hat{k}} &= \frac{k k}{k^2}; \\ \hat{B}_{2,\hat{k}} &= \frac{k^2 \theta^2}{\theta k_{\theta} \theta k} - (- 1) \frac{k_{\theta}}{\theta k} + \frac{k_{\phi}}{\theta k} ; \end{aligned} \quad (43)$$

and $P_{}(x)$ denote -th order Legendre polynomials.

A. Angular Averaging

To proceed, we perform the angular averaging in Eq. (40) (i.e., integration over all directions of \hat{k}) analytically. In order to do this we note that Eq. (40), after substituting Eq. (42), is invariant to the simultaneous rotation of the vectors k , q , and \hat{n} . This means that after integrating over q , Eq. (40) must have the form

$$\begin{aligned} L_{ij}(; 2) &= \int d\hat{k} M_{ij;\hat{k}}(k; \hat{k} \cdot \hat{n}) \\ &= \int d\hat{n} M_{ij;\hat{k}}(k; \hat{k} \cdot \hat{n}); \end{aligned} \quad (44)$$

where M is an appropriately defined matrix. Accordingly, we can change the integration over \hat{k} in favor of integrating over \hat{n} . Thus instead of having the direction \hat{n} fixed and all the other vector rotating, we will now choose the direction of k fixed, and rotate the other vectors. Note also that operator \hat{L} does not depend on \hat{n} , and only the matrices B_{ij} are averaged upon. Thus Eq. (40) can be written as

$$L_{ij}(; 2) = \int \frac{dq}{(2)^3} L(\hat{k}; q) q^{-2} \mathfrak{B}_{ij,\hat{k}}(\hat{k}; q); \quad (45)$$

where

$$\begin{aligned} \mathfrak{B}_{ij,\hat{k}}(\hat{k}; q) &= \int d\hat{n} B_{i,\hat{k}}(\hat{k}) B_{j,\hat{k}}(q) \\ &= 4(2 + 1) k^{-1} q^{-1} \hat{B}_{i,\hat{k}} \hat{B}_{j,\hat{k}} k^{-1} q^{-1} P_{}(\hat{k} \cdot \hat{q}); \end{aligned} \quad (46)$$

Here we used the definition (42) and the following property of the Legendre polynomials

$$\int d\hat{n} P_{}(\hat{n} \cdot \hat{k}) P_{}(\hat{n} \cdot \hat{q}) = 4(2 + 1) P_{}(\hat{k} \cdot \hat{q}); \quad (47)$$

Now, using Eq. (43) we can write the matrices explicitly:

$$L_{ij}(\hat{k}; \hat{q}) = P_k^0 P_k^0 P_q^0 P_q^0 \sim_{ij}^0 \hat{k}; \hat{q}; \quad (48)$$

where

$$\sim_{11}(\hat{k}; \hat{q}) = P(\hat{k}; \hat{q}); \quad (49)$$

$$\sim_{12}(\hat{k}; \hat{q}) = \sim_{21}(\hat{q}; \hat{k}) = \int_0^h {}^2P(\hat{k}; \hat{q}) \hat{k} \hat{q} P^0(\hat{k}; \hat{q}) + \hat{k} \hat{k} P^0(\hat{k}; \hat{q}); \quad (50)$$

$$\begin{aligned} \sim_{22}(\hat{k}; \hat{q}) = & \int_0^h {}^4P(\hat{k}; \hat{q}) (2^2 - 1) \hat{k} \hat{q} P^0(\hat{k}; \hat{q}) + (\hat{k} \hat{q})^2 P^0(\hat{k}; \hat{q}) + (\hat{k} \hat{k} + \hat{q} \hat{q}) P^0(\hat{k}; \hat{q}) \\ & + \hat{q} \hat{q} \hat{k} \hat{k} P^{(IV)}(\hat{k}; \hat{q}) + \hat{k} \hat{k} + \hat{q} \hat{q} \int_0^h ({}^2 - 1) P^0(\hat{k}; \hat{q}) \hat{k} \hat{q} P^{(III)}(\hat{k}; \hat{q}) \\ & + \hat{q} \hat{k} P^{(III)}(\hat{k}; \hat{q}); \end{aligned} \quad (51)$$

B. Transform to 2-dimensional Integral

Examining Eq. (40) we recall that the matrix $L_{ij}(\hat{k}; \hat{q})$ contains an integration over p , cf. Eq. (29). This integration is relatively trivial because of the existence of the δ -function. We can integrate over p simply expressing p as $p = k - q$. Next we integrate over q in spherical coordinates. Since we fixed the direction of k , we can choose it, without loss of generality, in the direction of the z axis. Then,

$$L_{ij}(\hat{k}; \hat{q}) = \int_0^{Z+1} q^2 dq \int_0^Z \sin \theta d\theta \int_0^{Z-2} d\Gamma_{ij}(\hat{k}; \hat{q}); \quad (52)$$

It can be shown that $\Gamma_{ij}(\hat{k}; \hat{q}) = \Gamma_{ij}(\hat{k}; \hat{q}; \cos \theta)$, i.e. does not depend on angle θ . So, we obtain a 2-dimensional integral

$$L_{ij}(\hat{k}; \hat{q}) = \int_0^{Z+1} q^2 dq \int_1^{Z+1} da \Gamma_{ij}(\hat{k}; \hat{q}; a); \quad (53)$$

where $a = \cos \theta$.

One more remark: the kernel in Eq. (40) is symmetric with respect to permuting the vectors q and p . This

means that we can actually integrate not over all q -space, but only over half-space, namely, when $q < p = \sqrt{k^2 + 2akq + q^2}$. This not only decreases the calculation time, but also allows us not to integrate near the point $p = 0$, where the kernel is in general singular.

C. Window of Locality

In performing the integration numerically we need to worry about the convergence of the integrand. Convergence is guaranteed only within a given interval of the scaling exponent ν which is referred to as the "window of locality". To find the window of locality one should expand the kernel in Eq. (53) for both small and large q and investigate its behavior at these regions. It is a straightforward (but cumbersome) procedure, and we show explicit results of such an expansion only near $q = 0$ for $\nu = 4$ and the 'exponential' decay model (22). Also we choose here $k = 1$, exploiting the homogeneity of all our operators in k . The equations satisfied by $\Gamma_{ij}(\hat{k} = 1; \hat{q}; a)$ are:

$$\begin{aligned} q^2 \Gamma_{1;1} &= \frac{5}{216} a (1 - a^2) (3 - 30a^2 + 35a^4) q^3 - 2 + \frac{5}{288} a (1 - a^2) (3 - 30a^2 + 35a^4) q^{11=3-2} \\ &+ \frac{1}{648} (1 - a^2) (3 - 52a^2) (3 - 30a^2 + 35a^4) q^4 - 2 + \frac{5}{432} a (1 - a^2) (3 - 30a^2 + 35a^4) q^{13=3-2} + O(q^{14=3-2}); \\ q^2 \Gamma_{1;2} &= \frac{5}{18} a (1 - 6a^2 + 5a^4) q^3 - 2 + \frac{5}{144} a (1 + 9a^2 - 45a^4 + 35a^6) q^{11=3-2} \\ &+ \frac{1}{108} (1 - a^2) (51 - 494a^2 + 835a^4) q^4 - 2 + \frac{5}{144} a (1 + 21a^2 - 55a^4 + 35a^6) q^{13=3-2} + O(q^{14=3-2}); \\ q^2 \Gamma_{2;1} &= \frac{5}{18} a (3 + 30a^2 - 55a^4 + 28a^6) q^3 - 2 + \frac{5}{24} a (3 + 30a^2 - 55a^4 + 28a^6) q^{11=3-2} \\ &+ \frac{1}{108} (1 - a^2) (9 + 426a^2 - 3105a^4 + 3080a^6) q^4 - 2 + \frac{5}{36} a (3 + 30a^2 - 55a^4 + 28a^6) q^{13=3-2} + O(q^{14=3-2}); \end{aligned} \quad (54)$$

$$q^2 \mathbb{L}_{2;2} = \frac{5}{6} a (13 - 30a^2 + 17a^4) q^3 - \frac{5}{3} a (1 - a^2)^2 (4 + 7a^2) q^{11=3-2} - \frac{1}{18} (1 - a^2) (96 + 89a^2 + 155a^4) q^4 - \frac{5}{24} a (1 - a^2) (19 - 71a^2 + 56a^4) q^{13=3-2} + O(q^{14=3-2}) \quad (55)$$

After integration over $a = \cos \theta$ we obtain

$$\begin{aligned} \int_{-1}^1 da q^2 \mathbb{L}_{1;1} &= \frac{832}{25515} q^4 - \frac{2}{3} + O(q^{14=3-2}); \quad (56) \\ \int_{-1}^1 da q^2 \mathbb{L}_{1;2} &= \frac{832}{2835} q^4 - \frac{2}{3} + O(q^{14=3-2}); \\ \int_{-1}^1 da q^2 \mathbb{L}_{2;1} &= \frac{4544}{8505} q^4 - \frac{2}{3} + O(q^{14=3-2}); \\ \int_{-1}^1 da q^2 \mathbb{L}_{2;2} &= \frac{4544}{945} q^4 - \frac{2}{3} + O(q^{14=3-2}); \end{aligned}$$

It is clear that integrals have IR divergence if $\nu_2 > 5$.

This result may seem surprising, since the original kernel in Eq. (40) has terms that depend on q as q^{-2} . Each of these terms begins to diverge if $\nu_2 > 3$. There is, however, a cancellation of the leading terms, resulting in an increase in the IR limit of the window of locality, up to the $\nu_2 = 4$. The subleading terms turn out to be antisymmetric in a , always vanishing after the angular integration. Thus the actual limit of the window of locality is as computed above.

The situation is even more complicated for the next anisotropic sector $\ell = 6$. The next subleading term (sub-subleading), which gives the main IR contribution in the case $\ell = 4$, also vanishes after integration. This is due to the fact that the matrix elements \mathbb{L}_{ij} contain Legendre polynomials $P_\ell(a)$ as multipliers; these are orthogonal to all a^n , $n < \ell$, and the highest order of a in the term $q^{m-2} a^n$, Eq. (54), can not be greater than $m + 2$. So, one can conclude that the integrals converge in IR regime up to $\nu_2 < (\ell) = \ell + 1$, for $\ell \geq 4$. For $\ell = 4$ we have $\nu_2 = 5$.

The UV boundary of the window of locality also moves if ℓ increased, for the same reasons.

D. Integrals near the IR Edge of the Window of Locality: approximate calculation of the exponents

It is clear from Eq. (56) that each integral near the critical point $\nu_2 = 5$ (but $\nu_2 < 5$) has the form

$$\mathbb{L}_{ij}(\nu_2) = \frac{i_{ij}}{\nu_2} + f_{ij}(\nu_2); \quad (57)$$

where i_{ij} are given by the main coefficients in Eq. (56), and $f_{ij}(\nu_2)$ are regular functions near the point $\nu_2 = 5$.

The main observation is that

$$\det(i_{ij}) = i_{1;1} i_{2;2} - i_{1;2} i_{2;1} = 0; \quad (58)$$

ie. the determinant of the leading (divergent) parts of the integrals vanishes. This occurs equally well for $\ell = 4$ and $\ell = 6$, independently of decay model. Thus the full determinant can be written as

$$\det(\mathbb{L}_{ij}) = \frac{i_{1;1} i_{2;2} + i_{2;2} i_{1;1} - i_{1;2} i_{2;1} - i_{2;1} i_{1;2}}{\nu_2^2} + O(i_{1;1} i_{2;2} - i_{1;2} i_{2;1}); \quad (59)$$

Thus the determinant diverges in general at $\nu_2 = 5$. For $\nu_2 > 5$ the determinant is determined predominantly by the divergent term $1/\nu_2^2$.

We can use this fact to estimate the scaling exponents: in zeroth approximation one can use Eq. (59) with $i_{ij}(\nu_2)$ calculated exactly at the point $\nu_2 = 5$. The approximate value of scaling exponent is then

$$\nu_2 = 5 + \frac{i_{1;1} i_{2;2} + i_{2;2} i_{1;1} - i_{1;2} i_{2;1} - i_{2;1} i_{1;2}}{i_{1;1} i_{2;2} - i_{1;2} i_{2;1}}; \quad (60)$$

This estimate is valid only as long as $1/\nu_2^2 > 0$. Actually, the values of ν_2 estimated this way for both $\ell = 4$ and $\ell = 6$ and the two decay models yield $\nu_2 = 0.01 - 0.02$, validating the zeroth order approximation. It is possible, however, to calculate the determinant in this region exactly, as is done in the next subsections.

E. Calculating the Integrals near the IR Edge

Let us denote the integrands in Eq. (40) after the integration over $\cos \theta$ as $J_{ij}(q)$. Then we have

$$\mathbb{L}_{ij} = \int_0^{Z+1} J_{ij}(q) dq; \quad (61)$$

Let us also introduce

$$I_{ij}(q_0) = \int_{q_0}^{Z+1} J_{ij}(q) dq; \quad (62)$$

$$\bar{I}_{ij}(q_0) = \int_0^{q_0} J_{ij}(q) dq; \quad (63)$$

Then we have

$$\mathbb{L}_{ij} = I_{ij}(q_0) + \bar{I}_{ij}(q_0) \quad (64)$$

for an arbitrary q_0 .

For $q_0 \notin 0$ $I_{ij}(q_0)$ can be calculated numerically directly, because there are no singularities for $q \in 0$. (Note, and cf. Subsect. IV B, we integrate over half q -space, which does not include the second singular point

$p = \sqrt{k^2 + 2akq + q^2} = 0$). On the other hand, using Eq. (56) $I_{i,j}(q_0)$ for sufficiently small q_0 and l can be represented as

$$I_{i,j}(q_0) = I_{i,j} \frac{q_0^2}{2} + O(q_0^{2+3}) \quad (65)$$

and one obtains the following formula for the integral $L_{i,j}$:

$$L_{i,j} = L_{i,j}(q_0) = I_{i,j}(q_0) + I_{i,j} \frac{q_0^2}{2} : \quad (66)$$

The test of validity of this formula is the independence of $L_{i,j}(q_0)$ of q_0 .

We have computed $L_{i,j}$ using Eq. (66) with q_0 varying over a wide range. It turns out that $L_{i,j}(q_0)$ is practically independent of q_0 provided that $q_{max} > q_0 > q_{min}$, where:

$$\begin{aligned} l = 4 : & \quad q_{max} = 2 \cdot 10^4 ; q_{min} = 5 \cdot 10^4 ; \\ l = 6 : & \quad q_{max} = 2 \cdot 10^4 ; q_{min} = 2 \cdot 10^4 ; \end{aligned}$$

"Practically independent of" means that the integrals change in this region of q_0 by an amount that is smaller than the minimum error of integration, (and see next subsection for the estimate of this error).

For $q_0 > q_{max}$ the simple approximation for $I_{i,j}(q_0)$ is not valid. For $q_0 < q_{min}$ the error of integration starts to grow rapidly. This is connected with high-order cancellations and finite machine precision. So, for $l = 6$ we have a 4th-order cancellation, which means that any small error in the calculation (or representation) of the leading term will increase by the factor q_0^4 . The relative precision in presenting numbers on the machine is about 10^{-16} , so for $q_0 = q_{min}(l = 6) = 2 \cdot 10^4$ we have a principal (machine) relative error of about 0.1, and, of course, the error of integration is increased here.

F. Integration Method

To perform the integration over q we used a standard Simpson integration rule which gives errors of the order $f^{(4)}(x)h^4$ (here $f(x)$ – integrand, h – integration step).

Performing the integration over $a = \cos \theta$ we used a 9-point closed type Newton-Cotes integration formula with error of the order $f^{(10)}h^{10}$. We have to use such high-order integration formula because of high-order cancellation for $l = 4$ and $l = 6$. Simpler integration schemes amplify small relative errors in the integration of the leading terms (which should cancel after angular integration) causing great absolute errors for small q .

The precision of integration was estimated by integral recalculation with smaller step h , and the error was determined as the maximum difference between the integrals, calculated with steps h , $h/2$ and $h/4$.

The error in determining the scaling exponent was estimated as

$$\delta \alpha = \frac{\det(L_{i,j})}{\partial \det(L_{i,j}) / \partial \alpha} ;$$

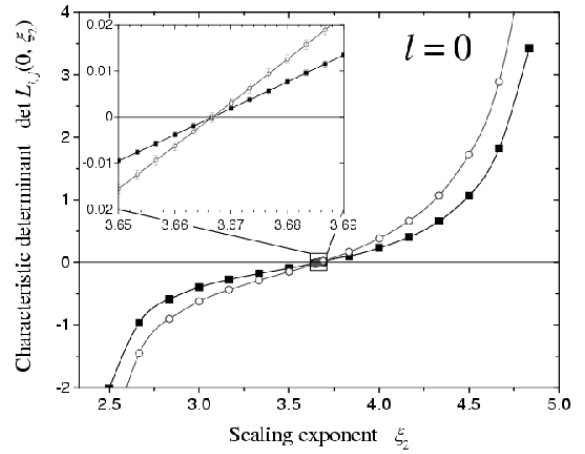


FIG. 1: determinant and zero crossing for the sector $l = 0$. The scaling exponent computed from the zero crossing is $\alpha_2(l = 0) = 0.667$.

where $\det(L_{i,j})$ is the accuracy of determining $\det(L_{i,j})$. We estimated $\delta \alpha_2 < 0.002$ in all cases.

V. RESULTS AND CONCLUDING REMARKS

The determinants $\det[L_{i,j}(l; \alpha_2)]$ were computed as a function of the scaling exponents α_2 in every l -sector separately, and the scaling exponent was determined from the zero crossing. The procedure is exemplified in Fig. 1 for the isotropic sector $l = 0$. We expect for this sector $\alpha_2(0) = 11/3$, in accordance with $\alpha_2(0) = 2/3$. Indeed, for both decay models, i.e. the exponential decay (22), shown in dark line, and the Gaussian decay (23) shown in light line, the zero crossing occurs at the same point, which in the inset can be read as 3.6667. For the higher l -sectors the agreement between the exponential and gaussian models is not as perfect, indicating that our procedure is not exact. In Fig. 2 we present the determinant and zero crossings for $l = 2$. From the inset we can read the exponents $\alpha_2(2) = 4.351$ and 4.366 for the exponential and Gaussian models respectively. This is in correspondence with $\alpha_2(2) = 1.351$ and 1.366 respectively. These numbers are in excellent correspondence with the experimental measurements reported in [5, 6]. The results for $l = 4$ are presented in Fig. 3. Here the zero crossing, as seen in the inset, yields very close results for $\alpha_2(4)$ between the exponential and Gaussian decay models, i.e. $\alpha_2(4) = 4.99$. Note that this result is very close to the boundary of locality as discussed in Subsect. IV C. Nevertheless the zero crossing is still easily resolved by the numerics, with the prediction that $\alpha_2(4) = 1.99$. We note that this number is well within the error bars of the simulational estimate of [9].

Similar results are obtained for $l = 6$, see Fig. 4. Also in this case exhibits zero crossing close to the boundary of locality, with $\alpha_2(6) = 6.98$. A gain we find close corre-

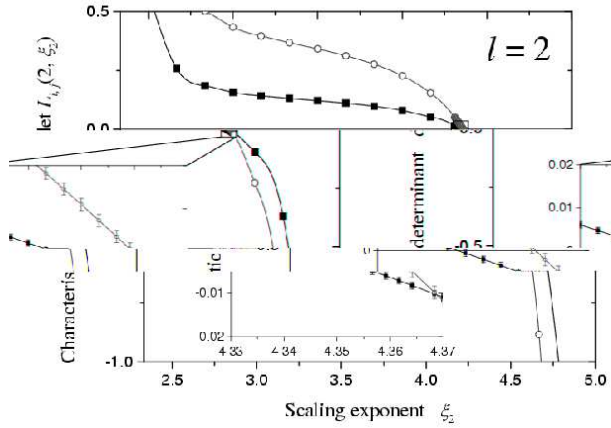


FIG. 2: determinant and zero crossing for the sector $\nu = 2$. The scaling exponent computed from the zero crossing is $\nu_2(\nu = 2) = 1.36 - 1.37$.

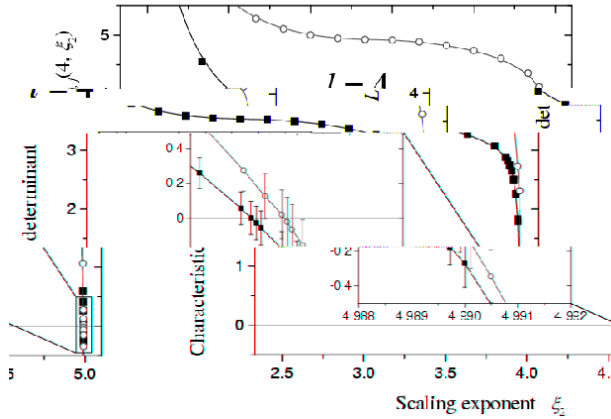


FIG. 3: determinant and zero crossing for the sector $\nu = 4$. The scaling exponent computed from the zero crossing is $\nu_2(\nu = 4) = 1.99$.

spontaneous between the exponential and Gaussian models. In terms of ν_2 this means $\nu_2(6) = 3.98$. This number appears higher than the simulation result of [9], which estimated $\nu_2(6) = 3.2$. We note however that for $\nu = 6$ the log-log plots of [9] scaled over less than half a decade, and improved simulations may well result in a substantial increase in the estimate.

Interestingly enough, the set of exponents $\nu_2(\nu) = 2/3, 1.36, 1.99$ and 3.98 for $\nu = 0, 2, 4$ and 6 respectively are in

close agreement with the numbers obtained for the linear pressure model, $\nu_2(\nu) = 2/3, 1.25226, 2.01922, 4.04843$, for $\nu = 0; 2; 4$ and 6 respectively. We reiterate at this point that the latter set is exact for the linear pressure model, whereas the former set is obtained within the DIA approximation. Nevertheless the close correspondence between the two leads us to propose that the actual exponents in the Navier-Stokes case must be very close to

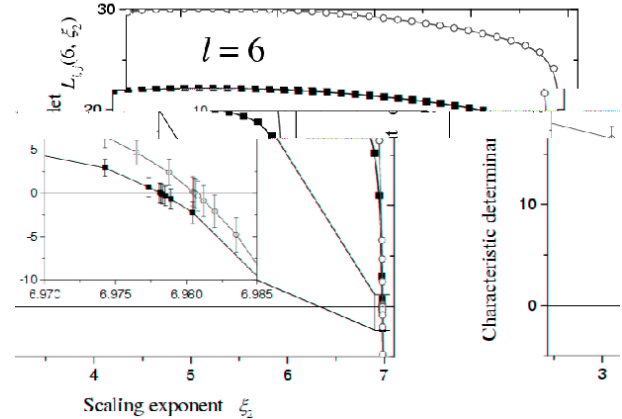


FIG. 4: determinant and zero crossing for the sector $\nu = 6$. The scaling exponent computed from the zero crossing is $\nu_2(\nu = 6) = 3.98$.

these predictions. We thus propose that careful experiments and simulations are likely to find the anisotropic exponents $\nu_2(\nu) \sim \nu/2$ for all $\nu > 2$, with about $2/3$ and $4/3$ for $\nu = 0$ and 2 respectively. If so, the restoration of isotropy at large Re and small scales should be quite clear, with high ν contributions decaying very rapidly, and the $\nu = 2$ contribution decaying with a gap exponent of about $2/3$. We do not expect a much more precise theoretical evaluation of these exponents before the intermittency problem in the isotropic sector is fully settled.

Acknowledgments

This work has been supported in part by the European Commission under a TM R grant, The Minerva Foundation, Munich, Germany, the German Israeli Foundation, the Israeli Science Foundation and the Naftali and Anna Backenroth-Bronicki Fund for Research in Chaos and Complexity.

- [1] A. Pumir and B. Shraiman, Phys. Rev. Lett. 75, 3114 (1995).
 [2] A. Pumir, Phys. Fluids 8, 3112 (1996).
 [3] S. Gary and Z. Warhaft, Phys. Fluids 10, 662 (1998).
 [4] I. Arad, V. S. L'vov and I. Procaccia, Phys. Rev. E 59,

- 6753 (1999).
 [5] I. Arad, B. Dhruva, S. Kurien, V. S. L'vov, I. Procaccia and K. R. Sreenivasan, Phys. Rev. Lett., 81, 5330 (1998).
 [6] S. Kurien, V. S. L'vov, I. Procaccia and K. R. Sreenivasan, Phys. Rev. E 61, 407 (2000).

- [7] S. Kurien and K. R. Sreenivasan, *Phys. Rev. E* **62**, 2206 (2000).
- [8] I. A rad, L. Biferale, I. Mazzitelli and I. Procaccia, *Phys. Rev. Lett.* **82**, 5040 (1999).
- [9] L. Biferale, I. Daumont, A. Lanotte and F. Toschi, preprint (2002).
- [10] I. A rad, L. Biferale and I. Procaccia, *Phys. Rev. E*, **61**, 2654 (2000).
- [11] I. A rad, V. S. L'vov, E. Podivilov and I. Procaccia, *Phys. Rev. E* **62**, 4901 (2000).
- [12] I. A rad and I. Procaccia, *Phys. Rev. E* **63**, 056302 (2001).
- [13] S. Grossmann, A. Heydt and D. Lohse, *J. Fluid. Mech.*, **440**, 381 (2001).
- [14] J. L. Lumley, *Phys. Fluids* **8**, 1056 (1967).
- [15] R. H. Kraichnan, *Phys. Fluids* **11**, 945 (1968).